Organic Electronics 32 (2016) 220–227

Contents lists available at ScienceDirect

Organic Electronics

journal homepage: www.elsevier.com/locate/orgel

Photo- and electroluminescence of ambipolar, high-mobility, donor-acceptor polymers

Martin Held [a], Yuriy Zakharko [a], Ming Wang [b], Florian Jakubka [b], Florentina Gannott [b], Joseph W. Rumer [c], Raja Shahid Ashraf [c], Iain McCulloch [c], Jana Zaumseil [a, *]

[a] Universität Heidelberg, Institute for Physical Chemistry, 69120 Heidelberg, Germany
[b] Friedrich-Alexander-Universität Erlangen-Nürnberg, Department of Materials Science and Engineering, 91058 Erlangen, Germany
[c] Imperial College London, Department of Chemistry and Centre for Plastic Electronics, London SW7 2AZ, UK

ARTICLE INFO

Article history:
Received 5 December 2015
Received in revised form
16 February 2016
Accepted 21 February 2016
Available online 4 March 2016

Keywords:
Donor-acceptor polymers
Ambipolar
Field-effect transistors
Electroluminescence
Photoluminescence
Polaron quenching

ABSTRACT

Donor-acceptor polymers with narrow bandgaps are promising materials for bulk heterojunction solar cells and high-mobility field-effect transistors. They also emit light in the near-infrared. Here we investigate and compare the photoluminescence and electroluminescence properties of different narrow bandgap (<1.5 eV) donor-acceptor polymers with diketopyrrolopyrrole (DPP), isoindigo (IGT) and benzodipyrrolidone (BPT) cores, respectively. All of them show near-infrared photoluminescence quantum yields of 0.03–0.09% that decrease with decreasing bandgap. Bottom-contact/top-gate field-effect transistors show ambipolar charge transport with hole and electron mobilities between 0.02 and 0.7 $cm^2 V^{-1} s^{-1}$ and near-infrared electroluminescence. Their external quantum efficiencies reach up to 0.001%. The effect of polaron quenching and other reasons for the low electroluminescence efficiency of these high mobility polymers are investigated.

1. Introduction

Donor-acceptor polymers based on diketopyrrolopyrrole (DPP) and other large core units (e.g. indigo, isoindigo, cyclopenta[2,1-*b*:3,4-*b*′]dithiophene, indaceno[1,2-*b*:5,6-*b*′]dithiophene) have attracted considerable attention over the past few years [1]. Due to the donor-acceptor hybridization of alternating electron-rich and electron-poor repeat units and the extended HOMO and LUMO distribution along their backbone these polymers exhibit a narrow bandgap (HOMO-LUMO gap) of less than 1.5 eV. Consequently, they were initially pursued for their ability to absorb near-infrared light as the donor layer in bulk heterojunction photovoltaic cells [2]. Many of these semiconducting polymers also show field-effect mobilities above 1 $cm^2 V^{-1} s^{-1}$ despite a lack of significant long-range order [3]. The origin of the high carrier mobility appears to be the reduction of torsional freedom and thus nearly disorder-free transport [4]. Due to their narrow bandgap and low-lying LUMO levels these polymers often show not only hole but also electron transport with comparable mobilities [5], which makes them interesting candidates for ambipolar and also light-emitting field-effect transistors (LEFETs) [6]. Ambipolar LEFETs combine the high current and charge carrier densities of field-effect transistors with the emission properties of light-emitting diodes. However, due to their planar structure they allow for spatial control of the emission zone, complete recombination of holes and electrons in a single layer and thus maximized quantum efficiencies [7–9].

Although the photophysical properties of donor-acceptor polymers have been studied extensively with regard to absorption, exciton generation and charge separation [10], their properties as near-infrared (NIR) light emitters have only recently been considered for NIR light-emitting diodes [11–13]. Near-infrared light has many applications from telecommunication, night-vision to biological imaging. However, efficient organic NIR emitters, especially beyond 900 nm, are scarce. While there are many highly efficient organic emitters for visible light a significant drop of photoluminescence yield is observed for molecules that emit at wavelengths above 700 nm [14] and alternative solution-processable NIR emitters such as quantum dots and carbon nanotubes may need to be used [15–17]. High mobility polymers would be attractive for LEFETs if they could combine their high carrier mobilities with high emission efficiencies in order to achieve maximum exciton density and brightness [12,18,19]. The high

* Corresponding author.
E-mail address: zaumseil@uni-heidelberg.de (J. Zaumseil).

http://dx.doi.org/10.1016/j.orgel.2016.02.030

mobilities found for many donor-acceptor polymers are promising but their emission properties are yet unknown.

Here we investigate the photoluminescence and electroluminescence properties of four exemplary donor-acceptor polymers (DPPT-TT, DPPT-BT, IGT-T and BPT-T) as shown in Fig. 1. All of these semiconducting polymers exhibit ambipolar charge transport with good mobilities [3,5,20,21]. They have different optical bandgaps and different donor and acceptor units that may change their emission properties. We use ambipolar LEFETs in a bottom-contact/top-gate geometry to obtain electroluminescence spectra and external quantum efficiencies (EQE) for these polymers at high current densities and find a strong dependence of photoluminescence (PL) and electroluminescence (EL) efficiencies on the HOMO-LUMO gap of the polymer. We discuss fast non-radiative decay and polaron quenching as possible origins for the observed low electroluminescence efficiencies.

2. Experimental

2.1. Materials

The semiconducting polymers DPPT-TT (poly(2,5-*bis*(2-octyldodecyl)-3,6-*di*(thiophen-2-yl)diketopyrrolo[3,4-*c*]pyrrole-1,4-dione-*alt*-thieno[3,2-*b*]thiophene), $M_n = 23$ kg/mol, $M_w = 87$ kg/mol) and DPPT-BT (poly(2,5-*bis*(2-octyldodecyl)-3,6-*di*(thiophen-2-yl)diketopyrrolo[3,4-*c*]pyrrole-1,4-dione-*alt*-benzo[*c*][1,2,5]thiadiazole), $M_n = 33$ kg/mol, $M_w = 87$ kg/mol) were purchased from Flexink Ltd. IGT-BT (poly((*E*)-4,4′-*bis*(2-octyldodecyl)[6,6′-bithieno[3,2-*b*]pyrrolylidene]-5,5′-dione-*alt*-benzo[*c*][1,2,5]thiadiazole), $M_n = 40$ kg/mol, $M_w = 60$ kg/mol) and BPT-T (poly(1,5-*bis*(2-octyldodecyl)-3,7-*di*(thiophen-2-yl)pyrrolo[2,3-*f*]indole-2,6-dione-*alt*-thiophene), $M_n = 34$ kg/mol, $M_w = 57$ kg/mol) were synthesized as described previously [20,21].

2.2. Film characterization

Polymer films and solutions were prepared as detailed in supplementary information S1. Absorption spectra of thin films and solutions were recorded with a Cary 6000i UV/Vis/NIR absorption spectrometer (Varian). Near-infrared photoluminescence (PL) spectra were recorded with an Acton SpectraPro SP2358 spectrometer (grating 150 lines/mm) and a liquid nitrogen-cooled InGaAs line camera (PI Acton OMA V:1024 1.7). For PL quantum yield (QY) measurements a 785 nm laser beam was directed through the entrance port of an integrating sphere (Spectralon coating) while polymer solutions in quartz cuvettes and thin film samples, respectively, were positioned in the center of the sphere. Quantum yield measurements were performed according to DeMello et al. [22]. The scattered laser light and PL signal were fiber-coupled to the spectrometer. Emission spectra were compared to PL spectra measured outside the sphere to account for reabsorption/reemission effects in the integrating sphere [23]. To verify the reliability of our QY measurements, we also estimated the QY of a well-known near-infrared standard IR-26 Dye (Acros Organics) in 1,2-dichloromethane. The obtained value of 0.15% was at the upper limit of reported values [24,25]. EL and PL spectra were corrected against the response of the detection system with a calibrated tungsten halogen lamp.

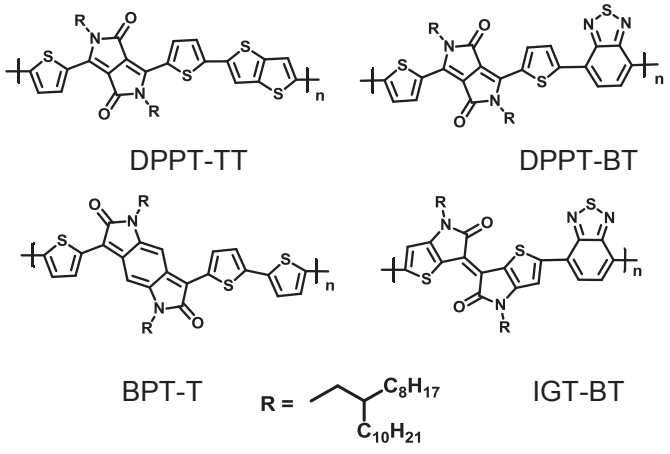

Fig. 1. Molecular structures of DPPT-TT, DPPT-BT, BPT-T and IGT-BT.

2.3. Light emitting transistor characterization

Bottom-contact (Cr/Au)/top-gate (Ag) field-effect transistors on glass with a PMMA or a hybrid (PMMA/HfO_2 [26]) dielectric were used. Detailed information about device fabrication can be found in the supplementary information S1. Current-voltage characteristics were recorded with an Agilent 4156C Semiconductor Parameter Analyzer or a Keithley 2612A source meter. Gate dielectric capacitances were measured with an Agilent E4980A Precision LCR Meter.

Electroluminescence images were recorded with a thermoelectrically cooled 256 × 360 pixel InGaAs camera (Xenics XEVA-CL-TE3, 800–1600 nm). PL and EL spectra were obtained with the same spectrometer as described above. For PL measurements a 640 nm (20 mW) or a 785 nm (10 mW) laser diode (OBIS, Coherent Europe B.V.) were used for excitation. The laser was focussed onto the channel area through a near-infrared ×50 or ×100 objective (Olympus LCPLN50XIR, NA 0.65 with correction collar or LMPlan100XIR, NA 0.8), which also collected PL/EL emission. A cold mirror (750 nm) and a long-pass filter rejected scattered laser light. All PL and EL spectra were smoothed and normalized.

The total light output in the near-infrared was measured with a calibrated InGaAs photodiode (Thorlabs FGA21-CAL, active area 3.1 mm^2) positioned underneath the transistor to enable collection of most of the emitted light. The silver gate electrode acted as a back mirror. The external quantum efficiency (EQE) defined as the number of outcoupled photons divided by the number of injected charges was calculated from the maximum photocurrent I_{diode} of the photodiode (at 0 V bias) during a sweep of the gate voltage for constant drain current (I_d) according to:

$$EQE = \frac{I_{diode}}{I_d} \cdot \frac{\int EL_{norm}(\lambda)\mathrm{d}\lambda}{\int S(\lambda)\cdot EL_{norm}(\lambda)\mathrm{d}\lambda} \cdot \frac{e}{hc} \cdot \frac{\int \lambda \cdot EL_{norm}(\lambda)\mathrm{d}\lambda}{\int EL_{norm}(\lambda)\mathrm{d}\lambda} \quad (1)$$

with $S(\lambda)$ as the wavelength-depended sensitivity of the photodiode weighted by the normalized $EL(\lambda)$ spectrum of the respective polymer.

3. Results and discussion

3.1. Photoluminescence

For basic characterization the absorption spectra of dilute solutions, as-spun and annealed films were recorded (see supplementary information S2) but did not change much for any of the polymers. The absorption onset in solution was blue-shifted compared to the films in all cases, as is common for conjugated polymers. Yet, the shift was minimal and indicates either only small conformational changes of the polymer backbones from solution to the solid state or just increased π-π-stacking. In addition, DPPT-TT

and DPPT-BT showed a vibronic shoulder that became more prominent with annealing. The absorption onset of the annealed films was used to determine the optical bandgap, as shown in Table 1. IGT-BT was found to degrade very quickly when exposed to air as observed by changing absorption spectra over time. This is most likely due to the relatively high HOMO level of IGT-BT (see supplementary information Table S1) and thus sensitivity to oxidation.

The photoluminescence spectra of dilute solutions, as-cast thin films and annealed thin-films for all four polymers are shown in Fig. 2. They are rather broad (full width at half maximum of about 300 nm) with Stokes shifts between 50 and 130 nm and fully within the near infrared region (>700 nm). The PL spectra of IGT-BT and BPT-T in solution could not be recorded reliably due to their low emission efficiency and strong reabsorption. IGT-BT thin films degraded too quickly for any PL measurements. The DPPT-TT and DPPT-BT thin-film spectra show a significant increase of the low energy shoulder compared to solutions, which is another indicator for increased order and chain planarization in the solid state. The emission dip around 800 nm in the short wavelength region of the DPPT-TT solution PL spectrum is a result of self-absorption.

The measured photoluminescence quantum yields (PL QY) for all polymers (except IGT-BT) in solution and as thin films are listed in Table 1. In all cases the QY is higher in solution than in the solid state. Annealing of the as-cast films leads to further although slight reduction of PL QY. These are also common observations for most conjugated polymers and are usually explained with the formation of excimers or non-emissive aggregate states, which is consistent with increased π-π-stacking and the observed red-shift [27–29].

Overall the quantum yields are very low with values between 0.28% for DPPT-TT in solution and 0.03% for BPT-T thin films. These low quantum yields may be partially attributed to the presence of sulfur atoms and the resulting spin–orbit coupling, which leads to increased formation of non-emissive triplets [30]. For this small set of polymers the quantum yield also decreases with decreasing bandgap. A similar trend was shown by Mayerhöffer et al. for squaraine near-infrared dyes [14]. Attempts to measure the fluorescence lifetime of the polymer films with a time-correlated single photon counting setup resulted in the same signal (at 1000 nm) as the instrument response function with a width of 90 ps (supplementary information S3). Accordingly, the lifetime is expected to be much shorter. This result is in agreement with reports by Cho et al. who measured lifetimes of 7 ps for DPPT-BT by transient absorption spectroscopy [31]. Such short total fluorescence lifetimes combined with the very low quantum yields indicate that the exciton decay in these polymers is dominated by very fast non-radiative decay.

3.2. Charge transport

All of the examined polymers show ambipolar transport without any current hysteresis in bottom-contact/top-gate transistors with a PMMA dielectric, as demonstrated by the transfer characteristics in Fig. 3 and previously reported for these polymers in various other device geometries [20,21,31,32]. Their small bandgaps, the position of the HOMO and LUMO levels (see Table S1) with respect to the work function of gold, as well as the employed top-gate structure all facilitate injection of both holes and electrons. Nevertheless, many devices still show non-ohmic contact effects at low source-drain voltages (V_{ds}, see supplementary information S4). The resulting contact resistance has to be kept in mind when calculating the field-effect mobilities. Table 2 summarizes saturation and linear mobilities and onset voltages for holes and electrons in transistors with a thick PMMA gate dielectric. The linear mobilities are lower in some cases than the respective saturation mobilities, which points toward contact effects. All mobilities increase slightly with gate voltage. We do not observe any peak of the apparent mobility close to the turn-on voltage, which sometimes results from gate voltage dependent contact resistance [33].

Although all polymers exhibit high mobilities for both charge carriers, the ratio of hole to electron mobility varies substantially. For DPPT-TT the hole mobility (0.68 $cm^2\ V^{-1}\ s^{-1}$) is more than ten times higher than the electron mobility (0.037 $cm^2\ V^{-1}\ s^{-1}$), while for DPPT-BT this ratio is reversed (0.035 $cm^2\ V^{-1}\ s^{-1}$ and 0.34 $cm^2\ V^{-1}\ s^{-1}$, respectively). The same is true for the onset voltages for hole (−8 V versus −21 V) and electron transport (24 V versus 6 V) of DPPT-TT and DPPT-BT, respectively. These differences can be partially explained by the much higher electron affinity of DPPT-BT (−3.8 eV) compared to DPPT-TT (−3.4 eV) (see Table S1). BPT-T and IGT-BT show overall lower but more balanced hole and electron mobilities. The onset voltage for hole transport for IGT-BT is positive, which corroborates its sensitivity to oxygen doping even under inert processing conditions due to its low ionization energy. This fact is also reflected in the high electron trap density calculated from the subthreshold swing for IGT-BT field-effect transistors (see supplementary information S5).

3.3. Electroluminescence

The top-gate transistors based on all four polymers showed electroluminescence (EL) in the ambipolar regime as a result of electron-hole-recombination in the channel. A narrow emission zone could be observed whose width (3.1 μm for thick PMMA and 1.7 μm for hybrid dielectric) exceeded the resolution limit of our setup (~1.3 μm). Its position was controlled by the gate voltage V_g and could be moved through the entire channel. Fig. 4a shows the intensity and position of near-infrared emission for a sweep in constant current mode for a DPPT-TT transistor with a thin hybrid dielectric. In constant current mode the drain current is fixed while the gate voltage is swept and the source-drain voltage varies accordingly. Note that emission is also observed next to the electrodes in the unipolar transport regime. This is likely to be due to injection of opposite charge carriers into the deep tail states of the polymer. Emission in the unipolar regime was described by Roelofs et al. for a related DPP-copolymer [34]. Due to the imbalance of carriers and incomplete recombination the quantum efficiency is

Table 1
Photophysical properties of DPPT-TT, DPPT-BT, BPT-T and IGT-BT. The optical band gap of the annealed thin films was calculated from the absorption onset of spincoated films. The PL quantum yield was determined for excitation at 785 nm.

	E_g^{opt} ann. film (eV)	Abs. peak solution (nm)	PL peak solution (nm)	Abs. peak ann. film (nm)	PL peak ann. film (nm)	PL QY in solution	PL QY as-spun film	PL QY ann. film
DPPT-TT	1.26	809	922	814	948	0.28%	0.09%	0.08%
DPPT-BT	1.18	935	989	945	1032	0.08%	0.06%	0.05%
BPT-T	1.03	990	–	969	1090	–	0.03%	0.03%
IGT-BT	0.87	1067	–	1044	–	–	–	–

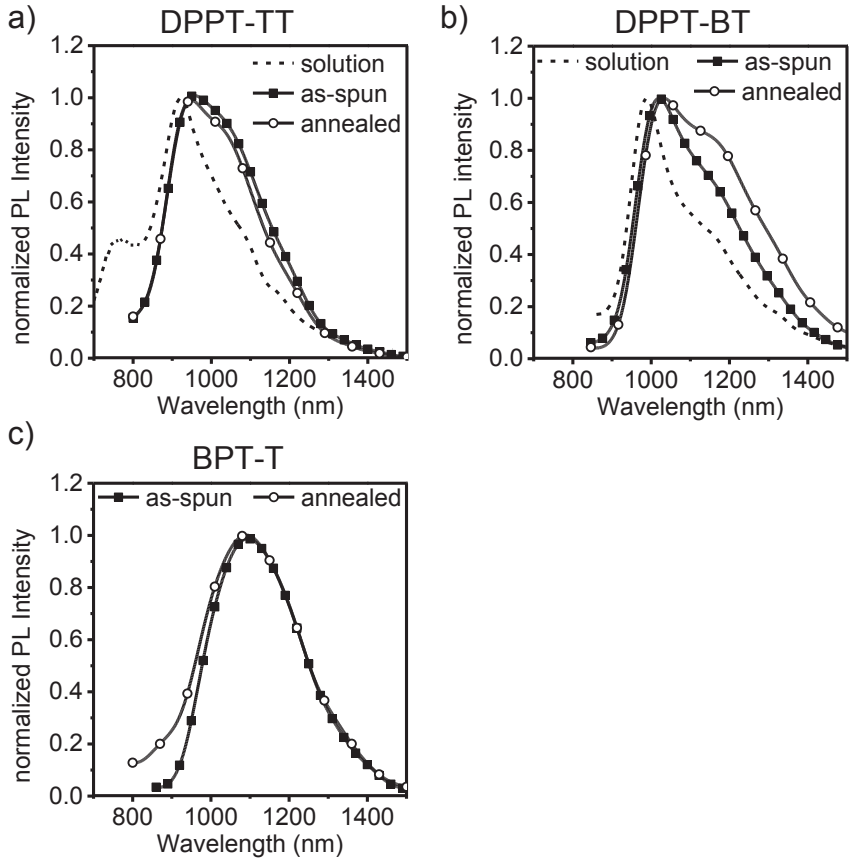

Fig. 2. Photoluminescence spectra of solutions, as-spun films and annealed films of (a) DPPT-TT, (b) DPPT-BT and (c) BPT-T.

very low in the unipolar regime. Balanced hole and electron recombination takes place in the ambipolar regime when the emission zone is located in the channel and away from the electrodes. Under these conditions the number of injected holes and electrons is exactly equal [8] and thus a constant emission intensity with maximum efficiency is expected for a constant current, leading to a plateau of the optical output power as shown in Fig. 4b.

Fig. 5 shows the EL and PL spectra from the channel region for DPPT-TT, DPPT-BT and BPT-T transistors. For DPPT-TT the EL spectra do not differ significantly from the PL spectra in the device. A slight red-shift in the EL of DPPT-BT may indicate preferential charge transport through more ordered regions of the polymer similar to observations by Noriega et al. for regioregular poly(3-hexylthiophene) [35]. We note that PL and EL spectra in multilayer devices such as LEFETs show a dependence of the overall stack thickness as demonstrated for various dielectric thicknesses for DPPT-TT transistors (see supplementary information S6) and hence comparison with single layer PL spectra is difficult.

Finally, the external quantum efficiency (EQE) for all devices was determined using gate voltage sweeps in constant current mode. The optical output is recorded during the sweep as shown in Fig. 4b and its plateau value for each drain current and thus various current densities was used to calculate the EQE according to equation (1). Fig. 6 shows the external quantum efficiencies for a number of different devices. The current density values were estimated by assuming an accumulation layer thickness of 1 nm. The dielectric (thick PMMA or thin PMMA/HfO_2 hybrid) did not have an effect on the maximum EQE for a given current density.

Several observations are noteworthy. The external efficiencies of all four different polymer LEFETs are much lower than expected. Even taking into account the singlet-triplet ratio and losses by waveguiding and reabsorption the highest EQE of DPPT-TT with 0.001% is very low compared to the PL QY of 0.08% in the annealed films. NIR light-emitting diodes beyond 850 nm typically exhibit electroluminescence efficiencies of 0.02–0.05% [12]. While the PL QY in thin films only vary by a factor of two to three between the polymers the EQEs differ by orders of magnitude. Further, for DPPT-TT the EQE seems to increase slightly with increasing current density while that of DPPT-BT stays roughly constant and that of BPT-T decreases.

4. Discussion

The band gaps of the four semiconducting polymers decrease according to the sequence DPPT-TT, DPPT-BT, BPT-T and IGT-BT. The PL quantum yield and external quantum efficiency of the LEFETs both decrease with the decreasing band gap but the electroluminescence shows a much stronger dependence. The reduced PL efficiency can be explained by the narrow bandgap. Non-radiative decay via vibrational modes becomes more likely as the energy differences between the excited state and the ground state is reduced and thus the number of necessary vibrational quanta.

Several factors are usually considered for reduced electroluminescence efficiency. Those are singlet-singlet annihilation, singlet-triplet quenching, polaron absorption and polaron quenching. The singlet exciton densities in our LEFETs are too low for singlet-singlet quenching as confirmed by the linear scaling of the PL intensity at different excitation powers well above the observed electroluminescence intensities. Triplets have much longer lifetimes than singlets and are formed in a 3:1 ratio by electron-hole recombination, which can lead to a strong increase of the triplet concentration and thus singlet-triplet quenching within the

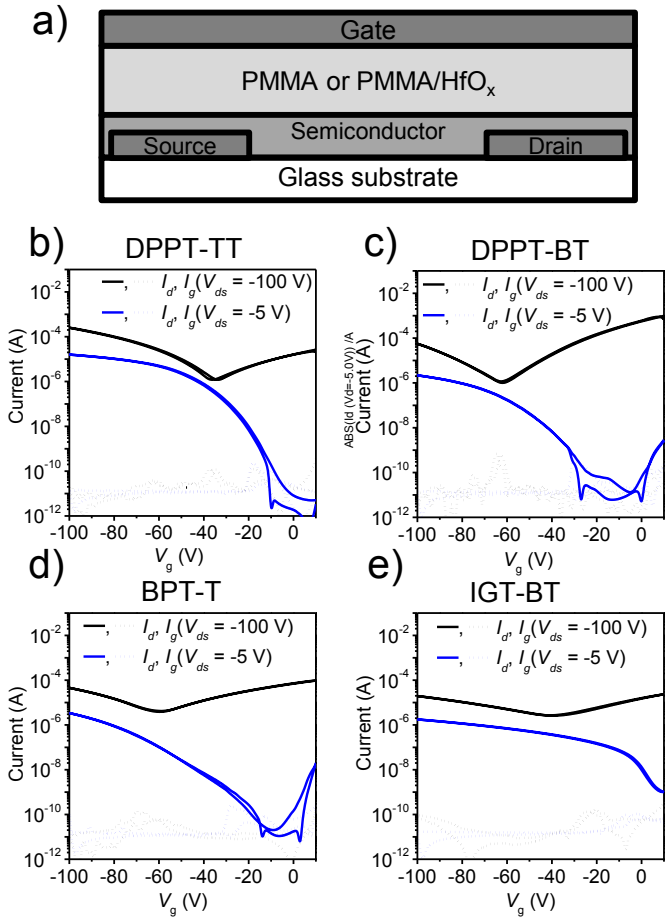

Fig. 3. (a) Schematic device structure of bottom-contact/top-gate transistors. Transfer characteristics of transistors with a thick PMMA dielectric (channel W/L = 125, L = 40 μm) of (b) DPPT-TT, (c) DPPT-BT, (d) BPT-T and (e) IGT-BT.

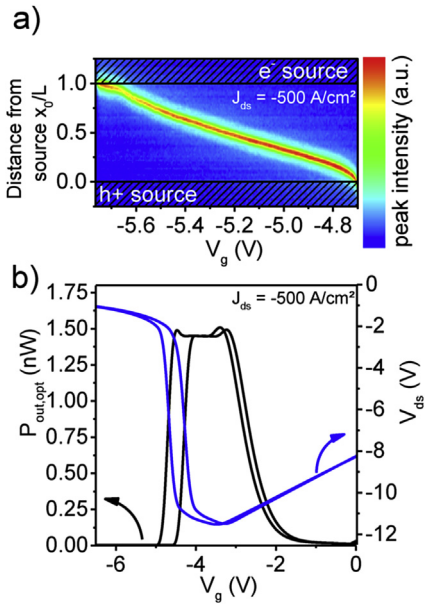

Fig. 4. (a) Position, width and intensity of the emission zone during a gate voltage sweep in constant current mode (current density J_{ds} = 500 A/cm^2) for a DPPT-TT transistor with a PMMA/HfO$_2$ hybrid dielectric. The source and drain electrodes are cross-hatched. (b) Optical output power and drain voltage versus gate voltage for a similar constant current sweep with J_{ds} = −500 A/cm^2.

recombination zone at high current densities. Relatively little is known about the exact photophysics of triplets in these donor-acceptor polymers. However, a recent study showed that the triplet lifetime of a polymer very similar to DPPT-TT (although with different alkyl sidechains) was unusually short with only 15 ns [36]. Although this is still much longer than the fluorescence lifetime (few ps), a significant concentration of triplets that could cause singlet-triplet quenching seems unlikely for our devices.

Due to the high charge carrier density in transistors compared to light-emitting diodes, polaron quenching must be considered as an important factor that could explain the low electroluminescence efficiency. Although, it is usually assumed that the recombination zone of an ideal LEFET is free of charge carriers this cannot be the case for real devices as the width of the recombination zone exceeds 1 μm and the recombination rate is not infinite [37,38]. Taking into account the substantially reduced bimolecular recombination rate that would be necessary for a recombination zone width of more than 1 μm, one finds that the sum of the electron and hole concentrations is not much lower than in the rest of the channel.

To determine the polaron quenching onset and to test whether the polarity of the charge carriers has an effect on the quenching of excitons, unipolar PL quenching measurements for DPPT-TT and DPPT-BT were performed (see supplementary information S7). The PL intensity dropped equally for accumulation of electrons or holes and thus quenching is equally strong for both charge carriers. The onset for polaron quenching can be estimated to occur for carrier densities of about 10^{18} to 10^{19} cm^{-3}, which is very similar to that for other conjugated polymers [39]. The carrier concentration for polaron quenching onset can vary between polymers and is somewhat lower for DPPT-BT than for DPPT-TT, which may explain the lower EQE for DPPT-BT transistors.

Gwinner et al. performed ambipolar PL quenching experiments with a low-mobility (<10^{-3} cm^2/V), green-emitting polyfluorene copolymer (F8BT) [9] and showed absence of PL quenching in the emission zone, which indicated at least very low carrier densities. We performed similar ambipolar PL quenching experiments on DPPT-TT and DPPT-BT transistors (see supplementary information S8). These did not only show a strongly quenched PL signal everywhere in the channel outside the recombination zone, but also non-negligible quenching within the recombination zone that increased with current density. Thus charge carriers (polarons) exist in the emission zone and can quench the formed excitons, which explains the lower than expected electroluminescence efficiencies.

Table 2
Saturation (μ_{sat}) and linear (μ_{lin}) field-effect mobilities and onset voltages (V_{on}) extracted from transfer characteristics for transistors with thick PMMA dielectric.

	$\mu_{sat,h}$ (cm^2 V^{-1} s^{-1})	$\mu_{lin,h}$ (cm^2 V^{-1} s^{-1})	$V_{on,h}$ (V)	$\mu_{sat,e}$ (cm^2 V^{-1} s^{-1})	$\mu_{lin,e}$ (cm^2 V^{-1} s^{-1})	$V_{on,e}$ (V)
DPPT-TT	0.68 ± 0.07	0.24 ± 0.005	−8.0 ± 3	0.037 ± 0.001	0.036 ± 0.001	24.0 ± 0.5
DPPT-BT	0.035 ± 0.01	0.015 ± 0.002	−21.0 ± 1	0.34 ± 0.12	0.13 ± 0.04	6.2 ± 0.2
BPT-T	0.092 ± 0.002	0.071 ± 0.002	−14.0 ± 0.5	0.074 ± 0.001	0.074 ± 0.002	4.5 ± 0.5
IGT-BT	0.018 ± 0.001	0.015 ± 0.002	7.1 ± 0.8	0.043 ± 0.003	0.04 ± 0.004	17.0 ± 1.0

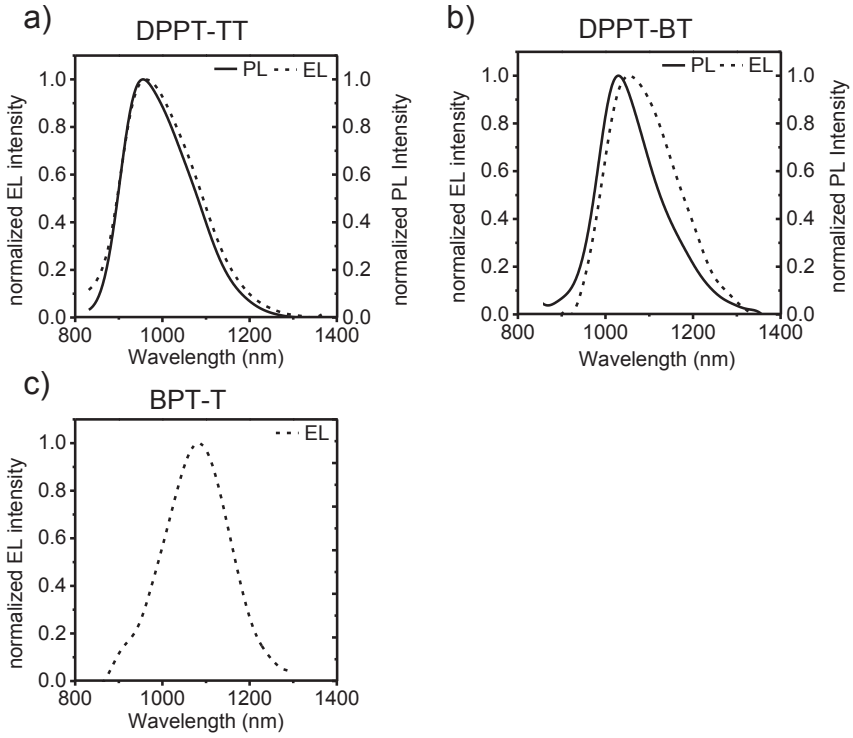

Fig. 5. Electroluminescence and photoluminescence spectra from the channel region of (a) DPPT-TT, (b) DPPT-BT and (c) BPT-T LEFETs. For BPT-T films within the device the PL spectra could not be measured without significant photobleaching and degradation.

Self-absorption and polaron absorption can further reduce the emission efficiency. The overlap of the absorption spectra of the uncharged polymers with the EL and PL spectra increases from DPPT-TT via DPPT-BT to BPT-T. The created photons must pass through approximately 29 nm of uncharged semiconductor. However, due to the relatively large Stokes-shift for all polymers, the expected self-absorption is insignificant. Moreover, charge accumulation spectroscopy [40] was performed (see supplementary information S9) to compare the polaron absorption spectra for all polymers. The EL spectrum fully overlaps with the polaron absorption spectrum in all cases, but the absorption cross section is relatively small and the presence of polarons in the recombination zone would only lead to an absorption of 2.5% of the emitted light and can also be neglected.

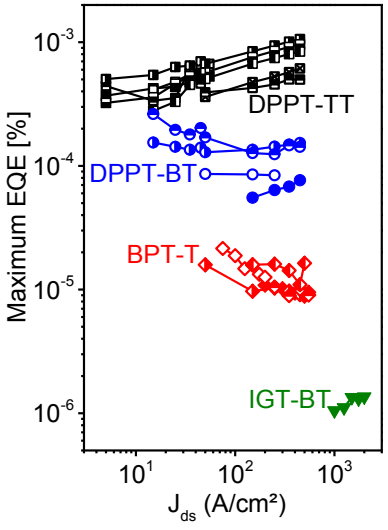

Fig. 6. Maximum external quantum efficiencies (EQE) of several LEFETs for each polymer versus estimated drain current density.

Consequently, the presence of polarons in the recombination zone is likely to be the main reason for the low EL efficiency of the investigated high mobility semiconductors. This notion is consistent with other high-mobility NIR-emitters, such as carbon nanotubes, for which emission from trions (charged excitons) in ambipolar transistors at high charge carrier densities [41] and in-situ Raman microscopy [42] also suggests the presence of charge carriers in the recombination zone. The question remains why this should be the case for these high-mobility polymers and not for the previously investigated low-mobility polymers like F8BT. There is increasing experimental evidence for reduced bimolecular recombination rates for a number of high mobility polymers in bulk heterojunction solar cells, although its origin is not clear [43–45]. Previous theoretical studies proposed that the recombination rate decreases with increasing anisotropic mobility [38], which would lead to broader emission zones and also higher concentrations of polarons within the recombination zone that would lead to quenching. The notion that high carrier mobilities may result in reduced recombination rate constants compared to the Langevin model and therefore cause broadened recombination zones would ultimately limit the achievable exciton density and brightness of ambipolar LEFETs due to increased instead of decreased polaron quenching. A solution for this problem could be multilayer structures that separate charge transport from emission [46,47]. Enhancement of the radiative decay rate via the Purcell effect of plasmonic nano-antennas might be another option to improve the efficiency of electroluminescent polymers in the NIR [48].

5. Conclusions

We investigated the photoluminescence and electroluminescence properties of four representative high-mobility donor-

acceptor polymers with different narrow bandgaps and emission in the near infrared beyond 850 nm. They showed low and decreasing photoluminescence yields with decreasing bandgaps and strongly declining electroluminescence efficiencies in ambipolar light-emitting field-effect transistors. The most likely reason for the lower than expected EQE appears to be polaron quenching within the recombination and emission zone of these ambipolar transistors due to a reduced bimolecular recombination rate. This effect would pose a serious limitation for the goal of high-current density, high-brightness LEFETs and may strengthen the case for suitable multilayer LEFETs.

Acknowledgment

This research was funded by European Research Council under the European Union's Seventh Framework Programme (FP/2007–2013)/ERC Grant Agreement No. 306298 (EN-LUMINATE). J.Z. also acknowledges general support by the Alfried Krupp von Bohlen und Halbach-Stiftung via the "Alfried Krupp Förderpreis für junge Hochschullehrer".

Appendix A. Supplementary data

Supplementary data related to this article can be found at http://dx.doi.org/10.1016/j.orgel.2016.02.030.

References

[1] S. Holliday, J.E. Donaghey, I. McCulloch, Advances in charge carrier mobilities of semiconducting polymers used in organic transistors, Chem. Mater. 26 (1) (2014) 647–663, http://dx.doi.org/10.1021/cm402421p.
[2] L. Huo, J. Hou, H.-Y. Chen, S. Zhang, Y. Jiang, T.L. Chen, Y. Yang, Bandgap and molecular level control of the low-bandgap polymers based on 3,6-dithiophen-2-yl-2,5-dihydropyrrolo[3,4- c]pyrrole-1,4-dione toward highly efficient polymer solar cells, Macromolecules 42 (17) (2009) 6564–6571, http://dx.doi.org/10.1021/ma9012972.
[3] Z. Chen, M.J. Lee, R. Shahid Ashraf, Y. Gu, S. Albert-Seifried, M. Meedom Nielsen, B. Schroeder, T.D. Anthopoulos, M. Heeney, I. McCulloch, H. Sirringhaus, High-performance ambipolar diketopyrrolopyrrole-thieno[3,2-b]thiophene copolymer field-effect transistors with balanced hole and electron mobilities, DPPT-TT, Adv. Mater. 24 (5) (2012) 647–652, http://dx.doi.org/10.1002/adma.201102786.
[4] D. Venkateshvaran, M. Nikolka, A. Sadhanala, V. Lemaur, M. Zelazny, M. Kepa, M. Hurhangee, A.J. Kronemeijer, V. Pecunia, I. Nasrallah, I. Romanov, K. Broch, I. McCulloch, D. Emin, Y. Olivier, J. Cornil, D. Beljonne, H. Sirringhaus, Approaching disorder-free transport in high-mobility conjugated polymers, Nature 515 (7527) (2014) 384–388, http://dx.doi.org/10.1038/nature13854.
[5] P. Sonar, S.P. Singh, Y. Li, M.S. Soh, A. Dodabalapur, A low-bandgap diketopyrrolopyrrole-benzothiadiazole-based copolymer for high-mobility ambipolar organic thin-film transistors, Adv. Mater. 22 (47) (2010) 5409–5413, http://dx.doi.org/10.1002/adma.201002973.
[6] L. Bürgi, M. Turbiez, R. Pfeiffer, F. Bienewald, H.-J. Kirner, C. Winnewisser, High-mobility ambipolar near-infrared light-emitting polymer field-effect transistors, Adv. Mater. 20 (11) (2008) 2217–2224, http://dx.doi.org/10.1002/adma.200702775.
[7] J. Zaumseil, R.H. Friend, H. Sirringhaus, Spatial control of the recombination zone in an ambipolar light-emitting organic transistor, Nat. Mater. 5 (1) (2006) 69–74, http://dx.doi.org/10.1038/nmat1537.
[8] J. Zaumseil, C.R. McNeill, M. Bird, D.L. Smith, P. Paul Ruden, M. Roberts, M.J. McKiernan, R.H. Friend, H. Sirringhaus, Quantum efficiency of ambipolar light-emitting polymer field-effect transistors, J. Appl. Phys. 103 (6) (2008) 64517, http://dx.doi.org/10.1063/1.2894723.
[9] M.C. Gwinner, D. Kabra, M. Roberts, Thomas J.K. Brenner, B.H. Wallikewitz, C.R. McNeill, R.H. Friend, H. Sirringhaus, Highly efficient single-layer polymer ambipolar light-emitting field-effect transistors, Adv. Mater. 24 (20) (2012) 2728–2734, http://dx.doi.org/10.1002/adma.201104602.
[10] L. Biniek, B.C. Schroeder, C.B. Nielsen, I. McCulloch, Recent advances in high mobility donor–acceptor semiconducting polymers, J. Mater. Chem. 22 (30) (2012) 14803, http://dx.doi.org/10.1039/c2jm31943h.
[11] M. Chen, E. Perzon, M.R. Andersson, S. Marcinkevicius, S.K.M. Jönsson, M. Fahlman, M. Berggren, 1 micron wavelength photo- and electroluminescence from a conjugated polymer, Appl. Phys. Lett. 84 (18) (2004) 3570, http://dx.doi.org/10.1063/1.1737064.
[12] T.T. Steckler, M.J. Lee, Z. Chen, O. Fenwick, M.R. Andersson, F. Cacialli, H. Sirringhaus, Multifunctional materials for OFETs, LEFETs and NIR PLEDs, J. Mater. Chem. C (2014), http://dx.doi.org/10.1039/c4tc00342j.
[13] G. Tregnago, T.T. Steckler, O. Fenwick, M.R. Andersson, F. Cacialli, Thia- and selena-diazole containing polymers for near-infrared light-emitting diodes, J. Mater. Chem. C 3 (12) (2015) 2792–2797, http://dx.doi.org/10.1039/C5TC00118H.
[14] U. Mayerhöffer, M. Gsänger, M. Stolte, B. Fimmel, F. Würthner, Synthesis and molecular properties of acceptor-substituted squaraine dyes, Chem. Eur. J. 19 (1) (2013) 218–232, http://dx.doi.org/10.1002/chem.201202783.
[15] G.J. Supran, K.W. Song, G.W. Hwang, R.E. Correa, J. Scherer, E.A. Dauler, Y. Shirasaki, M.G. Bawendi, V. Bulović, High-performance shortwave-infrared light-emitting devices using core-shell (PbS-CdS) colloidal quantum dots, Adv. Mater. Deerf. Beach Fla. 27 (8) (2015) 1437–1442, http://dx.doi.org/10.1002/adma.201404636.
[16] J. Schornbaum, Y. Zakharko, M. Held, S. Thiemann, F. Gannott, J. Zaumseil, Light-emitting quantum dot transistors: emission at high charge carrier densities, Nano Lett. 15 (3) (2015) 1822–1828, http://dx.doi.org/10.1021/nl504582d.
[17] F. Jakubka, C. Backes, F. Gannott, U. Mundloch, F. Hauke, A. Hirsch, J. Zaumseil, Mapping charge transport by electroluminescence in chirality-selected carbon nanotube networks, ACS Nano 7 (8) (2013) 7428–7435, http://dx.doi.org/10.1021/nn403419d.
[18] B.K. Yap, R. Xia, M. Campoy-Quiles, P.N. Stavrinou, Donal D.C. Bradley, Simultaneous optimization of charge-carrier mobility and optical gain in semiconducting polymer films, Nat. Mater. 7 (5) (2008) 376–380, http://dx.doi.org/10.1038/nmat2165.
[19] S.Z. Bisri, T. Takenobu, Y. Iwasa, The pursuit of electrically-driven organic semiconductor lasers, J. Mater. Chem. C 2 (16) (2014) 2827, http://dx.doi.org/10.1039/c3tc32206h.
[20] R.S. Ashraf, A.J. Kronemeijer, D.I. James, H. Sirringhaus, I. McCulloch, A new thiophene substituted isoindigo based copolymer for high performance ambipolar transistors, IGT-BT, Chem. Commun. 48 (33) (2012) 3939, http://dx.doi.org/10.1039/c2cc30169e.
[21] J.W. Rumer, M. Levick, S.-Y. Dai, S. Rossbauer, Z. Huang, L. Biniek, T.D. Anthopoulos, J.R. Durrant, D.J. Procter, I. McCulloch, BPTs: thiophene-flanked benzodipyrrolidone conjugated polymers for ambipolar organic transistors, BPT-T, BPT-2T, Chem. Commun. 49 (40) (2013) 4465, http://dx.doi.org/10.1039/c3cc40811f.
[22] John C. de Mello, H.F. Wittmann, R.H. Friend, An improved experimental determination of external photoluminescence quantum efficiency, Adv. Mater. 9 (3) (1997) 230–232, http://dx.doi.org/10.1002/adma.19970090308.
[23] T.-S. Ahn, R.O. Al-Kaysi, A.M. Müller, K.M. Wentz, C.J. Bardeen, Self-absorption correction for solid-state photoluminescence quantum yields obtained from integrating sphere measurements, Rev. Sci. Instrum. 78 (8) (2007) 86105, http://dx.doi.org/10.1063/1.2768926.
[24] A. Penzkofer, O. Lammel, T. Tsuboi, Emission spectroscopic characterisation of F2− colour centres in a LiF crystal, Opt. Commun. 214 (1–6) (2002) 305–313, http://dx.doi.org/10.1016/S0030-4018(02)02168-5.
[25] O.E. Semonin, J.C. Johnson, J.M. Luther, A.G. Midgett, A.J. Nozik, M.C. Beard, Absolute photoluminescence quantum yields of IR-26 Dye, PbS, and PbSe quantum dots, J. Phys. Chem. Lett. 1 (16) (2010) 2445–2450, http://dx.doi.org/10.1021/jz100830r.
[26] M. Held, S.P. Schießl, D. Miehler, F. Gannott, J. Zaumseil, Polymer/metal oxide hybrid dielectrics for low voltage field-effect transistors with solution-processed, high-mobility semiconductors, Appl. Phys. Lett. 107 (8) (2015) 83301, http://dx.doi.org/10.1063/1.4929461.
[27] M. Baghgar, J.A. Labastide, F. Bokel, R.C. Hayward, M.D. Barnes, Effect of polymer chain folding on the transition from H- to J-aggregate behavior in P3HT nanofibers, J. Phys. Chem. C 118 (4) (2014) 2229–2235, http://dx.doi.org/10.1021/jp411668g.
[28] R. Jakubiak, C.J. Collison, W.C. Wan, L.J. Rothberg, B.R. Hsieh, Aggregation quenching of luminescence in electroluminescent conjugated polymers, J. Phys. Chem. A 103 (14) (1999) 2394–2398, http://dx.doi.org/10.1021/jp9839450.
[29] T.-Q. Nguyen, I.B. Martini, J. Liu, B.J. Schwartz, Controlling interchain interactions in conjugated polymers: the effects of chain morphology on exciton–exciton annihilation and aggregation in MEH–PPV films, J. Phys. Chem. B 104 (2) (2000) 237–255, http://dx.doi.org/10.1021/jp993190c.
[30] S.C. Rasmussen, S.J. Evenson, C.B. McCausland, Fluorescent thiophene-based materials and their outlook for emissive applications, Chem. Commun. Camb. Engl. 51 (22) (2015) 4528–4543, http://dx.doi.org/10.1039/c4cc09206f.
[31] S. Cho, J. Lee, M. Tong, J.H. Seo, C. Yang, Poly(diketopyrrolopyrrole-benzothiadiazole) with ambipolarity approaching 100% equivalency, Adv. Funct. Mater. 21 (10) (2011) 1910–1916, http://dx.doi.org/10.1002/adfm.201002651.
[32] A.J. Kronemeijer, E. Gili, M. Shahid, J. Rivnay, A. Salleo, M. Heeney, H. Sirringhaus, A selenophene-based low-bandgap donor-acceptor polymer leading to fast ambipolar logic, Adv. Mater. 24 (12) (2012) 1558–1565, http://dx.doi.org/10.1002/adma.201104522.
[33] T. Uemura, C. Rolin, T.-H. Ke, P. Fesenko, J. Genoe, P. Heremans, J. Takeya, On the extraction of charge carrier mobility in high-mobility organic transistors, Adv. Mater. Deerf. Beach Fla. 28 (1) (2016) 151–155, http://dx.doi.org/10.1002/adma.201503133.
[34] W.S.C. Roelofs, W.H. Adriaans, R.A.J. Janssen, M. Kemerink, D.M. de Leeuw, Light emission in the unipolar regime of ambipolar organic field-effect transistors, Adv. Funct. Mater. (2013), http://dx.doi.org/10.1002/adfm.201203568 n/a.

[35] R. Noriega, J. Rivnay, K. Vandewal, Felix P.V. Koch, N. Stingelin, P. Smith, M.F. Toney, A. Salleo, A general relationship between disorder, aggregation and charge transport in conjugated polymers, Nat. Mater. (2013), http://dx.doi.org/10.1038/nmat3722.

[36] J.R. Ochsmann, D. Chandran, D.W. Gehrig, H. Anwar, P.K. Madathil, K.-S. Lee, F. Laquai, Triplet state formation in photovoltaic blends of DPP-type copolymers and PC71 BM, Macromol. Rapid Commun. 36 (11) (2015) 1122–1128, http://dx.doi.org/10.1002/marc.201400714.

[37] M. Kemerink, D.S.H. Charrier, E.C.P. Smits, S.G.J. Mathijssen, D.M. de Leeuw, R.A.J. Janssen, On the width of the recombination zone in ambipolar organic field effect transistors, Appl. Phys. Lett. 93 (3) (2008) 33312, http://dx.doi.org/10.1063/1.2963488.

[38] J. Zaumseil, C. Groves, J.M. Winfield, N.C. Greenham, H. Sirringhaus, Electron-hole recombination in uniaxially aligned semiconducting polymers, Adv. Funct. Mater. 18 (22) (2008) 3630–3637, http://dx.doi.org/10.1002/adfm.200800863.

[39] S. van Reenen, M.V. Vitorino, S.C.J. Meskers, R.A.J. Janssen, M. Kemerink, Photoluminescence quenching in films of conjugated polymers by electrochemical doping, Phys. Rev. B 89 (20) (2014), http://dx.doi.org/10.1103/PhysRevB.89.205206.

[40] R. Di Pietro, D. Fazzi, T.B. Kehoe, H. Sirringhaus, Spectroscopic investigation of oxygen- and water-induced electron trapping and charge transport instabilities in n-type polymer semiconductors, J. Am. Chem. Soc. 134 (36) (2012) 14877–14889, http://dx.doi.org/10.1021/ja304198e.

[41] F. Jakubka, S.B. Grimm, Y. Zakharko, F. Gannott, J. Zaumseil, Trion electroluminescence from semiconducting carbon nanotubes, ACS Nano 8 (8) (2014) 8477–8486, http://dx.doi.org/10.1021/nn503046y.

[42] S.B. Grimm, F. Jakubka, S.P. Schießl, F. Gannott, J. Zaumseil, Mapping charge-carrier density across the p-n junction in ambipolar carbon-nanotube networks by Raman microscopy, Adv. Mater. 26 (47) (2014) 7986–7992, http://dx.doi.org/10.1002/adma.201403655.

[43] S. Roland, M. Schubert, B.A. Collins, J. Kurpiers, Z. Chen, A. Facchetti, H. Ade, D. Neher, Fullerene-free polymer solar cells with highly reduced bimolecular recombination and field-independent charge carrier generation, J. Phys. Chem. Lett. 5 (16) (2014) 2815–2822, http://dx.doi.org/10.1021/jz501506z.

[44] B. Philippa, M. Stolterfoht, R.D. White, M. Velusamy, P.L. Burn, P. Meredith, A. Pivrikas, Molecular weight dependent bimolecular recombination in organic solar cells, J. Chem. Phys. 141 (5) (2014) 54903, http://dx.doi.org/10.1063/1.4891369.

[45] C.M. Proctor, M. Kuik, T.-Q. Nguyen, Charge carrier recombination in organic solar cells, Prog. Polym. Sci. 38 (12) (2013) 1941–1960, http://dx.doi.org/10.1016/j.progpolymsci.2013.08.008.

[46] M. Ullah, K. Tandy, S.D. Yambem, K. Muhieddine, W.J. Ong, Z. Shi, P.L. Burn, P. Meredith, J. Li, E.B. Namdas, Efficient and bright polymer light emitting field effect transistors, Org. Electron. 17 (2015) 371–376, http://dx.doi.org/10.1016/j.orgel.2014.12.014.

[47] R. Capelli, S. Toffanin, G. Generali, H. Usta, A. Facchetti, M. Muccini, Organic light-emitting transistors with an efficiency that outperforms the equivalent light-emitting diodes, Nat. Mater. 9 (6) (2010) 496–503, http://dx.doi.org/10.1038/nmat2751.

[48] Y. Zakharko, M. Held, F.-Z. Sadafi, F. Gannott, A. Mahdavi, U. Peschel, R.N.K. Taylor, J. Zaumseil, On-demand coupling of electrically generated excitons with surface plasmons via voltage-controlled emission zone position, ACS Photonics 3 (1) (2016) 1–7, http://dx.doi.org/10.1021/acsphotonics.5b00413.